Title	Joint unscented kalman filter for dual estimation in a bifilar pendulum for a small UAV
Author(s)	Ma, C; Chen, MZ; Lam, J; Cheung, KC
Citation	The 10th Asian Control Conference (ASCC 2015), Kota Kinabalu, Malaysia, 31 May-3 June 2015. In Conference Proceedings, 2015, p. 1-6
Issued Date	2015
URL	http://hdl.handle.net/10722/217501
Rights	Asian Control Conference. Copyright © IEEE.

Joint Unscented Kalman Filter for Dual Estimation in a Bifilar Pendulum for a Small UAV

Carlos Ma, Michael Z. Q. Chen, James Lam, and Kie Chung Cheung

***Abstract*—It has always been difficult to accurately estimate the moment of inertia of an object, e.g. an unmanned aerial vehicle (UAV). Whilst various offline estimation methods exist to allow accurate parametric estimation by minimizing an error cost function, they require large memory consumption, high computational effort, and a long convergence time. The initial estimate's accuracy is also vital in attaining convergence. In this paper, a new real time solution to the model identification problem is provided with the use of a Joint Unscented Kalman Filter for dual estimation. The identification procedures can be easily implemented using a microcontroller, a gyroscope sensor, and a simple bifilar pendulum setup. Accuracy, robustness, and convergence speed are achieved.**

***Index Terms*—Joint Unscented Kalman Filter, machine learning, model identification, dual estimation, UAV, quadrotor.**

I. Introduction

With the invention and the availability of low cost micro-electromechanical sensors (MEMS), microprocessors, and high energy density lithium-polymer (LiPo) batteries, small UAVs have been gaining much popularity amongst researchers, witnessing many innovative designs, applications, and theoretical developments [1] [2] [3]. To design an aggressive flight controller for a UAV, it is vital to have a firm knowledge on its moment of inertia I as it would affect how the aircraft rotates under an applied torque, and whether the rotations about the three principal axes are coupled. However, I is difficult to be identified for aircrafts with complex geometry.

One of the estimation methods is via computer aided design (CAD) modeling based on the parallel axis theorem [4] [5], which can be hard to realize as it may be very tedious to accurately model the aircraft with precision. Some of the experimental approaches include the use of forced or constrained rotation devices [6] [7] and free oscillations [5] [8] [9], often with the use of a suspension pendulum, e.g. the bifilar pendulum (Fig. 1) to be discussed in Section II-A. To identify system parameters in these platforms, one can either utilize numerical optimization techniques for accuracy or generate incomplete closed-form solutions for swiftness. This leads to a question: can a real-time solution be created to provide both advantages whilst utilizing only the readily available angular rate measurements of a UAV?

This work was supported by the National Natural Science Foundation of China under Grant 61374053, the SZSTI Basic Research Scheme under Grant JCYJ20120831142942514, Grant GRF HKU 7140/11E, and Grant GRF HKU 17200914. (Corresponding author: M. Z. Q. Chen.)

C. Ma, M. Z. Q. Chen, J. Lam, and K. C. Cheung are with the Department of Mechanical Engineering, The University of Hong Kong, Pokfulam, Hong Kong, and the Shenzhen Institute of Research and Innovation, University of Hong Kong, Shenzhen, China (e-mail: carlosma@hku.hk; mzqchen@hku.hk; james.lam@hku.hk; kccheung@hku.hk).

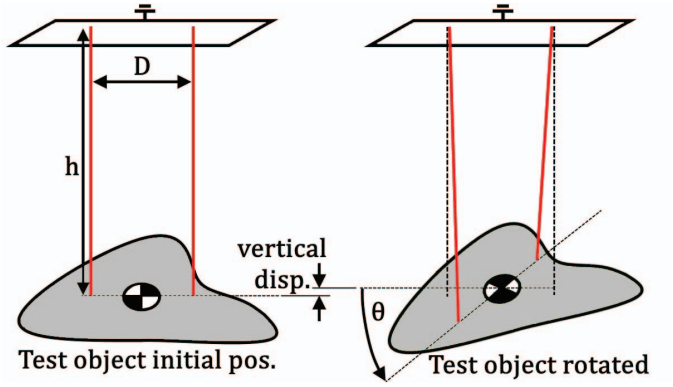

Fig. 1. A bifilar pendulum.

In this paper, a real-time algorithm based on the Joint Unscented Kalman Filter (JUKF) was developed to tackle the highly nonlinear dual estimation problem with the use of a bifilar pendulum. Its performance is compared with that of an Extended Kalman Filter (EKF) in simulations and experiments, showing superior performance and robustness in estimation.

II. Background

A. The Bifilar Pendulum

The bifilar pendulum is an unactuated experimental platform, primarily for the identification of the moment of inertia I of the suspended mass m. An initial twist is given to the mass, causing it to rotate and oscillate about the vertical axis. The equation describing the rotational dynamics of a bifilar pendulum [8] can be derived using the Lagrangian dynamics formulation as follows:

$$\begin{aligned}\ddot{\theta} &= -\left(\frac{mgD^2}{4Ih}\right)\frac{\sin\theta}{\sqrt{1+0.5(D/h)^2(\cos\theta-1)}} \\ &\quad -\frac{C_D}{I}\dot{\theta}|\dot{\theta}| - \frac{C_v}{I}\dot{\theta}, \end{aligned} \tag{1}$$

where θ, g, D, h, C_D, and C_v are the mass rotational displacement from its neutral position, gravitational acceleration, wire separation, wire length, coefficient of aerodynamic drag, and viscous damping coefficient, respectively. One may linearize Eq. (1) about $\theta = \dot{\theta} = 0$ and algebraically solve it to obtain $I = mgD^2T^2/(16h\pi^2)$, where T is the oscillation period. This expression is useful in giving a quick estimate on I but could give no information on the aerodynamic and viscous

978-1-4799-7862-5/15/$31.00 © 2015 IEEE

drags. The variables and constants to be estimated are now formulated as a state vector such that

$$x = \begin{bmatrix} x_1 & ... & x_5 \end{bmatrix}^T = \begin{bmatrix} \theta & \dot{\theta} & I & C_D & C_v \end{bmatrix}^T, \quad (2)$$

with constants m, g, D, h assumed to be known in advance and superscript T denoting the matrix transpose. The system can now be represented by a continuous-time model as $\dot{x} = f(x)$, such that $f = \begin{bmatrix} f_1 & f_2 & f_3 & f_4 & f_5 \end{bmatrix}^T$, in which

$$f_1 = x_2 \quad (3)$$

$$f_2 = -\left(\frac{mgD^2}{4x_3h}\right)\frac{\sin x_1}{\sqrt{1+0.5(D/h)^2(\cos x_1 - 1)}} - \frac{x_4}{x_3}x_2|x_2| - \frac{x_5}{x_3}x_2 \quad (4)$$

$$f_3 = f_4 = f_5 = 0. \quad (5)$$

Filters designed based on this state structure are usually titled with the prefix "Joint" in that they perform dual estimation using a single plant: it is omitted in the paper for brevity.

B. Kalman Filter

The discrete-time Kalman Filter (KF) [10] [11] [12] [13] is a recursive prediction-correction algorithm that minimizes the state estimate error covariance P_{xx} in the optimal case. The general formulation to the correction step can be summarized as follows:

$$K_{(k)} = P_{xz(k|k-1)}P^{-1}_{zz(k|k-1)} \quad (6)$$

$$x_{(k|k)} = x_{(k|k-1)} + K_{(k)}(z_{(k)} - z_{(k|k-1)}) \quad (7)$$

$$P_{xx(k|k)} = P_{xx(k|k-1)} - K_{(k)}P_{zz(k|k-1)}K^T_{(k)}, \quad (8)$$

where $x \in R^n$ is the state vector, $z \in R^m$ is the measurement vector, $P_{xx} \in R^{n\times n}$ is the state error covariance, $P_{xz} \in R^{n\times m}$ is the estimated measurement noise covariance, $P_{zz} \in R^{m\times m}$ is the actual measurement noise covariance, and $K \in R^{n\times m}$ is the Kalman gain. Subscript k represents the k^{th} time step, with $(k|k-1)$ denoting a priori estimate and $(k|k)$ denoting a posteriori estimate. Note that the KF only considers the propagation of the mean and covariance of x for operation, hence how well the recursive solution behaves depends on how well the two moments can be estimated [14]. The original linear KF (LKF) only works optimally in a linear system [10], whilst suboptimal variants such as the EKF [13] [15] and the UKF [16] were created to work with nonlinear systems.

1) Extended Kalman Filter: Without loss of generality, a nonlinear discrete-time system can be described as follows:

$$x_{(k)} = f(x_{(k-1)}) + B_v v_{(k-1)} \quad (9)$$

$$z_{(k)} = h(x_{(k)}) + w_{(k)}, \quad (10)$$

where $f : R^n \to R^n$ and $h : R^n \to R^m$ are differentiable functions and $v \in R^q$ and $w \in R^m$ are assumed to be white Gaussian noises with zero mean and covariances Q and R, i.e. $Q = E(vv^T)$ and $R = E(ww^T)$. It can be observed from the Taylor series of a nonlinear function that the mean and covariance can be estimated correctly up to the nth order if the variable distribution moments and the function derivatives are correct up to the nth order [14]. The EKF propagates the mean and covariances through [15]:

$$x_{(k|k-1)} = f(x_{(k-1|k-1)}) \quad (11)$$

$$z_{(k|k-1)} = h(x_{(k|k-1)}) \quad (12)$$

$$P_{xx(k|k-1)} = F_{(k-1)}P_{xx(k-1|k-1)}F^T_{(k-1)} + B_vQB^T_v \quad (13)$$

$$P_{xz(k|k-1)} = P_{xx(k|k-1)}H^T_{(k)} \quad (14)$$

$$P_{zz(k|k-1)} = H_{(k)}P_{xx(k|k-1)}H^T_{(k)} + R, \quad (15)$$

where $F_{(k-1)}$ and $H_{(k)}$ are the Jacobians of f and h. As a result, the mean and covariances will only be correct up to the first and second orders, which may cause divergence for some highly nonlinear functions. Also, the EKF cannot be applied to non-differentiable systems, e.g. those with time delay or hysteresis. Note that the noises are assumed to be additive, which is not required.

2) The Unscented Kalman Filter: Considering the same nonlinear discrete-time system as described by Eq. (9) and Eq. (10) with the noises treated as a part of the states (hence the nonlinear functions and covariances would be augmented), the UKF, at the beginning of each recursion, deterministically chooses a set of sigma points X_i with weight W_i and transforms them across the nonlinear plant models such that

$$X_{i(k)} = f(X_{i(k-1)}) \quad (16)$$

$$Z_{i(k)} = h(X_{i(k)}) \quad (17)$$

$$x_{(k|k-1)} = \sum_i W_i X_{i(k)} \quad (18)$$

$$z_{(k|k-1)} = \sum_i W_i Z_{i(k)} \quad (19)$$

$$P_{xx(k|k-1)} = \sum_i W_i (X_{i(k)} - x_{(k|k-1)})(X_{i(k)} - x_{(k|k-1)})^T \quad (20)$$

$$P_{xz(k|k-1)} = \sum_i W_i (X_{i(k)} - x_{(k|k-1)})(Z_{i(k)} - z_{(k|k-1)})^T \quad (21)$$

$$P_{zz(k|k-1)} = \sum_i W_i (Z_{i(k)} - z_{(k|k-1)})(Z_{i(k)} - z_{(k|k-1)})^T, \quad (22)$$

where $\sum_i W_i = 1$. It can be proven that both the mean and covariance of x can be propagated correctly up to the second order, and some higher-order terms can also be partially captured by using some specific sets of sigma points and weights [16]. The following set of $2n+1$ sigma points is used with the spread adjustment variable $\kappa = 3-n$: for $i = 1, ..., n$,

$$W_0 = \kappa/(\kappa + n) \quad (23)$$

$$W_{1:2n} = 1/(2(n + \kappa)) \quad (24)$$

$$X_{0(k-1)} = x_{(k-1|k-1)} \quad (25)$$

$$X_{i(k-1)} = x_{(k-1|k-1)} + (\sqrt{(n + \kappa)S})_i \quad (26)$$

$$X_{n+i(k-1)} = x_{(k-1|k-1)} - (\sqrt{(n + \kappa)S})_i, \quad (27)$$

where $(\sqrt{*})_i$ is the i^{th} column of the lower matrix square root of $*$ found by the Cholesky decomposition [17]. In summary,

the UKF estimates states and covariances more accurately than the EKF even for non-differentiable systems, whilst retaining the same order of computational load.

III. Problem statement and solution

A. The discrete-time bifilar pendulum model for recursive dual estimation

The simplest discrete-time bifilar pendulum model that incorporates the information of all state propagation is derived here by expanding the corresponding Taylor series and assuming constant angular acceleration at each time step, resulting in $x_{(k)} = g(x_{(k-1)}) + v$, where $g : R^5 \rightarrow R^5$. Therefore, $g = \begin{bmatrix} g_1 & g_2 & g_3 & g_4 & g_5 \end{bmatrix}^T$ with

$$g_1 = x_{1(k-1)} + f_{1(k-1)}\Delta t + f_{2(k-1)}\Delta t^2/2 + v_1 \quad (28)$$

$$g_2 = x_{2(k-1)} + f_{2(k-1)}\Delta t + v_2 \quad (29)$$

$$g_3 = x_{3(k-1)} + v_3 \quad (30)$$

$$g_4 = x_{4(k-1)} + v_4 \quad (31)$$

$$g_5 = x_{5(k-1)} + v_5, \quad (32)$$

and Δt denoting the sampling time of the filter. Note that the Jacobian of g can be easily found for the EKF and the value of Q for v is determined in Section III-B.

B. Kalman Filter Tuning

There are four parameters to be initialized in a KF, namely the initial state estimate $x_{(0)}$, the initial state error covariance $P_{xx(0)}$, the process noise covariance Q, and the measurement noise covariance R. Intuitively, $x_{(0)}$ and $P_{xx(0)}$ are closely related as they respectively determine the accuracy and precision of the initial estimate. Hence, if a very loose $x_{(0)}$ is applied, $P_{xx(0)}$ has to be large enough to cover the true state values. Given that the filter should be able to operate without having to know the actual initial angle and rotational speed, $x_{1(0)}$ and $x_{2(0)}$ are initialized to zero with the expectation that they would completely rely on the performance of the filter for convergence to the true values. For small objects, $x_{4(0)}$ and $x_{5(0)}$ are typically very small hence they are also initialized to zero. On the other hand, $x_{3(0)}$ can be initialized more accurately by the linearized solution of Eq. (1) or some simple CAD modeling, and if no pre-processing is desired, experiments have shown that for measuring the yaw mass moment of inertia of a small multicopter, $x_{3(0)}$ can be initialized as $x_{3(0)} \approx 0.5mr^2$ as a rough estimate, where r is the radius of the multicopter. It could also be initialized as some arbitrary value, e.g. $0.05\ \mathrm{kgm}^2$, provided that the corresponding entry in $P_{xx(0)}$ is large enough.

$P_{xx(0)}$ determines the initial precision of the state estimate and is tuned with respect to $x_{(0)}$ assuming no correlation in the initial errors, such that

$$P_{xx(0)} = \mathrm{diag}\left([E(e^2_{1(0)}), E(e^2_{2(0)}), E(e^2_{3(0)}), E(e^2_{4(0)}), E(e^2_{5(0)})]\right), \quad (33)$$

where $E(e^2_{i(0)})$ is the expected value of square of the error of the i^{th} initial state estimate. Since $x_{1(0)}$ and $x_{2(0)}$ were initialized as zero, $E(e^2_{1(0)})$ and $E(e^2_{2(0)})$ are set to be $\left(\frac{\pi}{2}\right)^2\ \mathrm{rad}^2$ and $(4\pi)\ \mathrm{rad}^2\mathrm{s}^{-2}$, respectively. Provided that $x_{3(0)}$ is estimated fairly accurately, $E(e^2_{3(0)})$ can be set fairly small, but it is experimentally proven to be a good practice to equate it to $x^2_{3(0)}$ to ensure a wide coverage of mass moment of inertia values. $E(e^2_{4(0)})$ and $E(e^2_{5(0)})$ are set to be 1 to cover a wide range of damping coefficients and to allow room for the filter to compensate for the initial angular and angular rate errors.

Following the above tuning procedure, the following set of x_0 and $P_{xx(0)}$ is found to provide convergence for a wide range of experimental setups without further tuning:

$$x_0 = \begin{bmatrix} 0 & 0 & 0.05 & 0 & 0 \end{bmatrix}^T \quad (34)$$

$$P_{xx(0)} = \mathrm{diag}\left(\begin{bmatrix} \frac{\pi}{2} & 4\pi & 0.05 & 1 & 1 \end{bmatrix}\right)^2. \quad (35)$$

The process noise Q determines how accurate the system model is with respect to the real model, hence it is expected that it would attain a higher norm for the EKF as the mean propagation is only accurate up to the first order as explained earlier. The entries of Q can be approximated by investigating the next most significant term in the corresponding Taylor series and assuming zero noise correlation, resulting in

$$Q = \mathrm{diag}\left(\left[\frac{\Delta t^3}{6}V_1, \frac{\Delta t^2}{2}V_1,\ \Delta t V_3, \Delta t V_4, \Delta t V_5\right]\right)^2, \quad (36)$$

where V_1 is the "maximum jerk" at each time step, experimentally identified to be $0.01\,\mathrm{ms}^{-3}$ for the UKF to provide a wide convergence range. As for the EKF, this parameter has to be re-tuned with respect to changes in the sampling time and measurement noise, no fixed value appeared to provide wide-range convergence. Noises V_3, V_4, V_5 are the "maximum rate of change" of the constants which should be kept low, but not zero, as that would mean no estimation capability of the three system constants. They are commonly set to be 10^{-5} in their respective units.

The measurement noise covariance R is measured by taking multiple samples of the sensor data and finding out the actual covariance. Note that the above parameters remain the same, unless otherwise specified.

IV. Experimental Setups and Results

Three experiments were conducted to compare the performance of linearization by Eq. (1), EKF, and UKF in dual estimation. The first experiment was numerically carried out in MATLAB/SIMULINK as a benchmark for the ideal performance of the listed methods. A steel rod with a known mass moment of inertia was used in the second experiment, whilst a small UAV was used in the third. Note that in the following experiments estimation exists for $t = 0\,\mathrm{s}$.

A. Experiment 1: Simulation

The bifilar pendulum simulator was built based on Eq. (1) to provide simulated noisy angular rate data for estimation. The performances of the different estimation solutions are compared and evaluated in two separate scenarios with varying system properties. Unless otherwise specified, the conditions given in Table I were used.

TABLE I
CONSTANTS AND CONDITIONS USED IN EXPERIMENT 1.

Constant	Value	Constant	Value
g	$9.80665\,\mathrm{ms}^{-2}$	$x_{2(0)\mathrm{true}}$	$0.2\,\mathrm{rads}^{-1}$
m	$0.5\,\mathrm{kg}$	$x_{3\mathrm{true}}$	$0.02\,\mathrm{kgm}^2$
D	$0.2\,\mathrm{m}$	$x_{4\mathrm{true}}$	$0.004\,\mathrm{kgm}^2\mathrm{rad}^{-1}$
h	$0.6\,\mathrm{m}$	$x_{5\mathrm{true}}$	$0.001\,\mathrm{kgm}^2\mathrm{s}^{-1}$
$x_{1(0)\mathrm{true}}$	$0.35\pi\,\mathrm{rad}$		

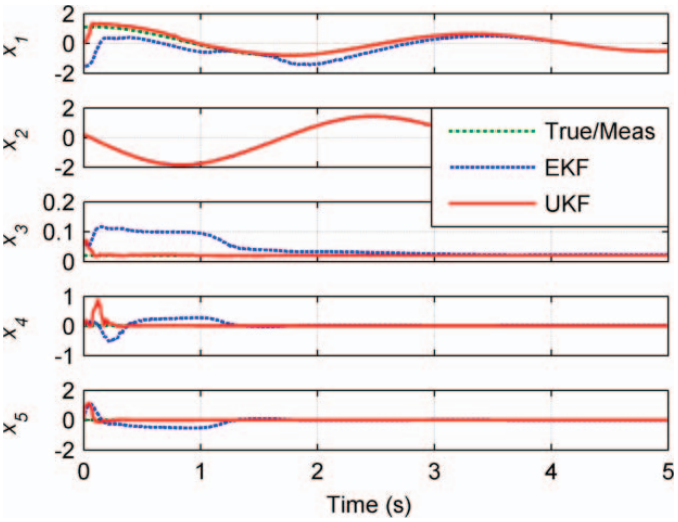

Fig. 2. Experiment 1A results with $\Delta t = 0.01\,\mathrm{s}$. "Maximum jerk" V_1 was set to be $1000\,\mathrm{ms}^{-3}$ for the EKF. The settings for the UKF were unaltered.

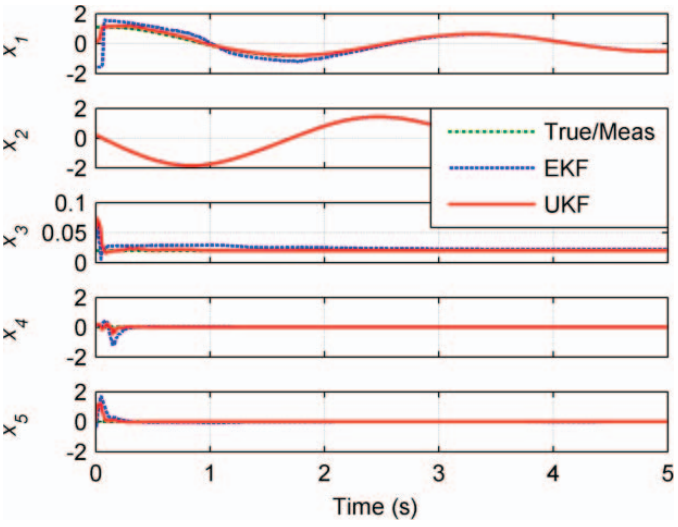

Fig. 3. Experiment 1B results with $\Delta t = 0.005\,\mathrm{s}$. "Maximum jerk" V_1 was set to be $1000\,\mathrm{ms}^{-3}$ for the EKF. The settings for the UKF were unaltered.

1) Varying sampling time: The simulation was first carried out at three sampling times, namely $\Delta t = [0.01, 0.005, 0.001]\,\mathrm{s}$ with the results shown in Figs. 2, 3, and 4. The final state estimates at $t = 5\,\mathrm{s}$ are also tabulated in Table II. The measurement noise was set to $10^{-4}\,\mathrm{rad}^2\mathrm{s}^{-2}$ in all cases and for the EKF V_1 was manually tuned for the best response.

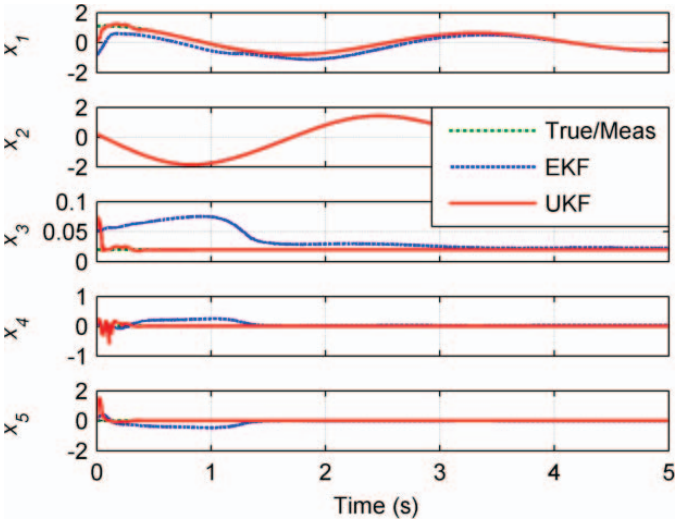

Fig. 4. Experiment 1C results with $\Delta t = 0.001\,\mathrm{s}$. "Maximum jerk" V_1 was set to be $60000\,\mathrm{ms}^{-3}$ for the EKF. The settings for the UKF were unaltered.

TABLE II
EXPERIMENT 1 DATA AT $t = 5\,\mathrm{s}$ IN THE CORRESPONDING UNITS.

$\Delta t = 0.01s$	Actual	Linear	EKF	UKF
x_3	0.0200	0.0204	0.0220	0.0201
x_4	0.0040	not available	0.0186	0.0041
x_5	0.0010	not available	-0.0083	0.0013
$\Delta t = 0.005s$	Actual	Linear	EKF	UKF
x_3	0.0200	0.0204	0.0219	0.0200
x_4	0.0040	not available	0.0049	0.0041
x_5	0.0010	not available	0.0018	0.0011
$\Delta t = 0.001s$	Actual	Linear	EKF	UKF
x_3	0.0200	0.0204	0.0224	0.0200
x_4	0.0040	not available	0.0263	0.0041
x_5	0.0010	not available	-0.0181	0.0010

From the results it can be observed that whilst simplified, linearization gave a fairly accurate estimate of the actual mass moment of inertia of the object, but it had no ability in identifying the drag properties at all. Comparing the responses from the EKF with that from the UKF, the following can be observed, 1) the angular rates converged almost instantaneously as the noise covariance for the measurement was relatively quite low, 2) the UKF converged much faster in all cases without further tuning, 3) an increase in the filter sampling frequency always improved the accuracy of the UKF, but such an improvement was not achievable in the EKF even after manual tuning, 4) due to the linearization in the EKF, the process noise covariance had to be set very large which is suspected to have caused the higher estimation bias present in the EKF estimates, 5) the mass moment of inertia converged the quickest in all cases, and its accuracy is seen to be related to that of the angle estimate, 6) there was transient energy gain indicated by the negative damping coefficients estimated before $t = 1\,\mathrm{s}$ to allow room for the angle and angular rate to converge, and 7) the EKF gave poorer performance at $\Delta t = 0.001\,\mathrm{s}$ when compared with its $\Delta t = 0.05\,\mathrm{s}$ counterpart.

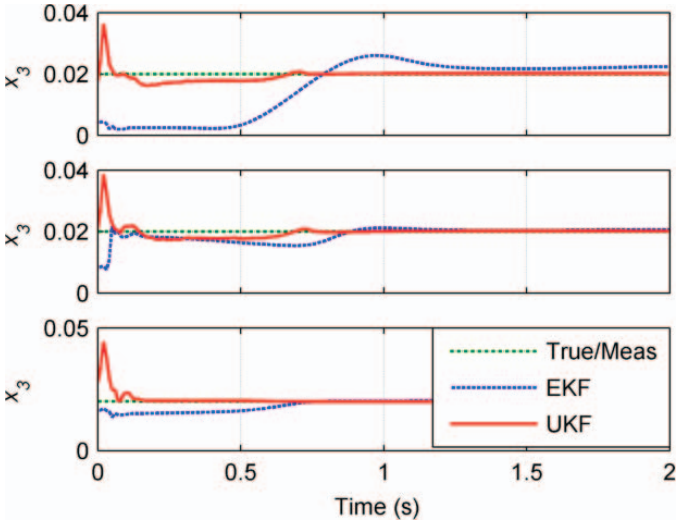

Fig. 5. Estimation of x_3 with different initial state estimates for the filters, from top to bottom: 0.2, 0.4, 0.8 of the actual constants and initial values.

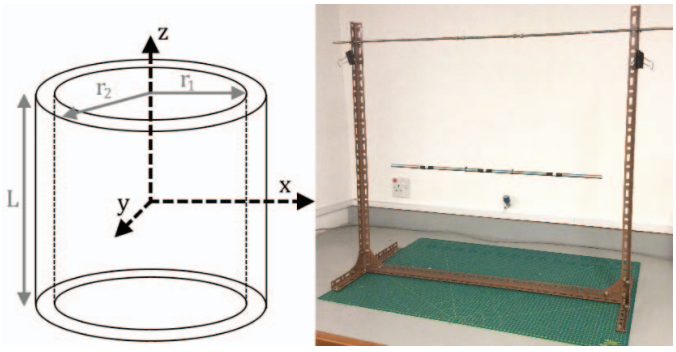

Fig. 6. A thick walled cylinder with mass m in a bifilar pendulum setup.

2) Varying initial estimates: The effects of the initial estimates given to the EKF and the UKF are investigated here with a fixed sampling time of $\Delta t = 0.01\,\mathrm{s}$ and a measurement noise covariance at $R = 10^{-9}\,\mathrm{rads}^{-1}$. "Maximum jerk" V_1 was fixed at 0.01 in the EKF for all three cases to allow an observation of the pure effects of the initial estimates, with the UKF's settings unaltered as before. The initial estimates given to the three trials are 0.2, 0.4, and 0.8 times the true initial conditions and values, generating the results of x_3 in Fig. 5, from which it can be observed that the UKF is more robust to the inaccuracy of the initial estimates than the EKF. In some cases when the initial estimates were far away from the actual values, the EKF diverged.

In summary, the EKF was very difficult to tune whilst the UKF dealt with nonlinearity and initial estimation uncertainty with greater robustness and consistency. It is further used in the following experiments on the physical platforms.

B. Experiment 2: Steel rod

The mass moment of inertia of an ideal thick wall cylinder (Fig. 6) about axis x is given by $I = \frac{1}{12}m[3(r_2^2 + r_1^2) + h^2]$, to which the UKF estimate should converge. The rod's

TABLE III
CONSTANTS USED IN EXPERIMENT 2.

Constant	Value	Constant	Value
m	$0.1678\,\mathrm{kg}$	r_1	$0.0039\,\mathrm{m}$
D	$0.15\,\mathrm{m}$	r_2	$0.005\,\mathrm{m}$
h	$0.4\,\mathrm{m}$	L	$0.67\,\mathrm{m}$

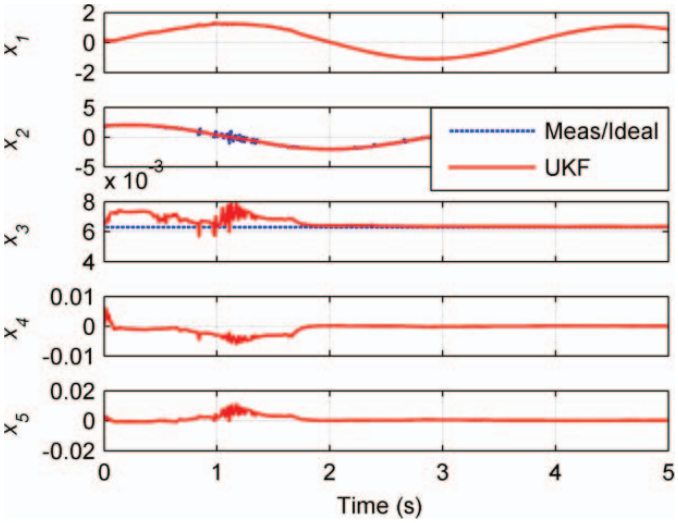

Fig. 7. UKF estimation for mass and drag properties of a steel rod in a bifilar pendulum.

angular recordings were tracked by a Flex13 tracking system then numerically differentiated to give angular rate readings. The constants of this experimental setup are given in Table III, where r_1, r_2, and L are the inner, outer radii and the length of the cylinder, respectively, resulting in $x_{3\mathrm{ideal}} = 6.28 \times 10^{-3}\,\mathrm{kgm}^2$. The following filter conditions were used in the UKF to obtain the results shown in Fig. 7:

$$\begin{aligned} \Delta t &= 0.01\,\mathrm{s} \\ x_{(0)} &= \begin{bmatrix} 0 & 0 & 0.006 & 0 & 0 \end{bmatrix}^T \\ P_{xx(0)} &= \mathrm{diag}\left(\begin{bmatrix} 0.5\pi & 4\pi & 0.005 & 0.01 & 0.01 \end{bmatrix}\right)^2 \\ R &= 0.02\,\mathrm{rad}^2\mathrm{s}^{-2}. \end{aligned}$$

From the results it can be observed that the UKF converged to the value found by the ideal equation of x_3 and oscillated about $6.32 \times 10^{-3}\,\mathrm{kgm}^2$. Although slightly different, the estimate given by the UKF is by no means less accurate than the one given by the ideal value as the rod may be bent or having non-uniform thickness and density, with extra mass given by the reflective tape and securing installations. States x_4 and x_5 converged to and oscillated about $1.66 \times 10^{-5}\,\mathrm{kgm}^2\mathrm{rad}^{-1}$ and $1.77 \times 10^{-4}\,\mathrm{kgm}^2\mathrm{s}^{-1}$ within the first few seconds, which should only be taken as a quick reference as such small values could be corrupted by the filter inaccuracy.

C. Experiment 3: UAV frame

Moving to the core demonstration of the use of UKF in this paper is the mass and drag estimation of a small UAV. Custom firmware was written for the microcontroller and sensors on

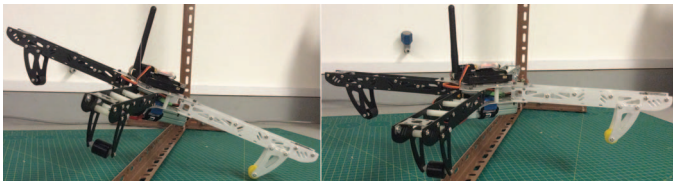

Fig. 8. Mounting the quadcopter onto the bifilar pendulum. Left and right pictures show a bad and good configuration, respectively.

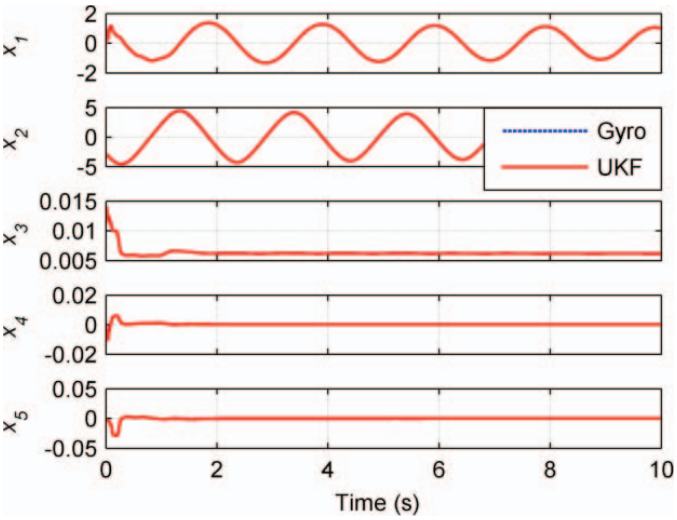

Fig. 9. UKF estimates for mass and drag properties of a small UAV frame.

the UAV to allow real time broadcasting of its gyroscopic data to the ground station, at which the UKF is implemented. This could have equally been done on the microcontroller itself but was avoided to allow ease in data recording. Before conducting the experiment, one has to make sure that the center of gravity (CG) of the quadcopter has to be directly below the plane created by the two filaments and equidistant between them, to avoid inaccurate estimation (Fig. 8). Note that the onboard accelerometer could be used as an inclinometer when mounting the quadcopter, to see if the aircraft is level. The following filter conditions and constants were used to obtain the results shown in Fig. 9:

$$
\begin{aligned}
m &= 0.485\,\mathrm{kg} \quad D = 0.195\,\mathrm{m} \quad h = 0.625\,\mathrm{m} \\
\Delta t &= 0.005 \\
x_{(0)} &= \begin{bmatrix} 0 & 0 & 0.01 & 0 & 0 \end{bmatrix}^T \\
P_{xx(0)} &= \mathrm{diag}\left(\begin{bmatrix} 0.5\pi & 4\pi & 0.01 & 0.01 & 0.01 \end{bmatrix}\right)^2 \\
R &= 3 \times 10^{-6}\,\mathrm{rad^2 s^{-2}}.
\end{aligned}
$$

After about $10\,\mathrm{s}$, x_3, x_4, and x_5 converged and oscillated about $6.18 \times 10^{-3}\,\mathrm{kgm^2}$, $1.41 \times 10^{-4}\,\mathrm{kgm^2 rad^{-1}}$, and $8.95 \times 10^{-5}\,\mathrm{kgm^2 s^{-1}}$, respectively. Note that $\hat{x}_3$ is quite low as the motors were not mounted on the frame, and again $\hat{x}_4$ and $\hat{x}_5$ should only be taken as a quick reference as they are very small. The reliability of $\hat{x}_4$ and $\hat{x}_5$ would increase for an aircraft with larger damping coefficients, e.g. a fixed wing aircraft with large lift surfaces. To measure the moments of inertia of the other axes, orient the aircraft accordingly. To further improve the accuracy of the estimates in the experiments, one may introduce better sensor measurements.

V. Conclusion

In conclusion, a real-time recursive algorithm based on the UKF has been developed to allow real-time identification of inertial and drag properties of a small UAV with the use of a bifilar pendulum. The proposed solution, in combination with the provided tuning procedure for the UKF, demands less memory, lower computational effort, and provides higher robustness than its offline numerical optimization counterparts, which requires offline data processing. Comparisons were made in between the results obtained from the linearization method, the EKF, and the UKF, and it was concluded that UKF was more robust and accurate in dual estimation, even given some very inaccurate initial guesses, with convergence achieved in a matter of seconds. Future investigations would include tri-axis simultaneous estimation.

References

[1] S. K. Phang, K. Li, K. H. Yu, B. M. Chen, and T. H. Lee, "Systematic design and implementation of a micro unmanned quadrotor system," *Unmanned Systems*, vol. 2, no. 02, pp. 121–141, 2014.

[2] K. Peng, G. Cai, B. M. Chen, M. Dong, K. Y. Lum, and T. H. Lee, "Design and implementation of an autonomous flight control law for a UAV helicopter," *Automatica*, vol. 45, no. 10, pp. 2333–2338, 2009.

[3] A. Kushleyev, D. Mellinger, C. Powers, and V. Kumar, "Towards a swarm of agile micro quadrotors," *Autonomous Robots*, vol. 35, no. 4, pp. 287–300, 2013.

[4] T. Jirinec, "Stabilization and control of unmanned quadcopter," Master's thesis, Czech Technical University in Prague, 2011.

[5] D. Zafirov, "Mass moments of inertia of joined wing unmanned aerial vehicle," *International Journal of Research in Engineering and Technology*, vol. 02, no. 12, pp. 325–331, December 2013.

[6] M. Da Lio, A. Doria, and R. Lot, "A spatial mechanism for the measurement of the inertia tensor: Theory and experimental results," *Journal of Dynamic Systems, Measurement, and Control*, vol. 121, no. 1, pp. 111–116, 1999.

[7] C. L. Bottasso, D. Leonello, A. Maffezzoli, and F. Riccardi, "A procedure for the identification of the inertial properties of small-size UAVs," in *XX AIDAA Congress*, 2009.

[8] M. R. Jardin and E. R. Mueller, "Optimized measurements of UAV mass moment of inertia with a bifilar pendulum," in *AIAA Guidance, Navigation and Control Conference and Exhibit*, 2007, pp. 20–23.

[9] M. R. Jardin, "Improving mass moment of inertia measurements," *MATLAB Digest*, 2010.

[10] R. E. Kalman, "A new approach to linear filtering and prediction problems," *Journal of Fluids Engineering*, vol. 82, no. 1, pp. 35–45, 1960.

[11] L. Xie and Y. C. Soh, "Robust Kalman filtering for uncertain systems," *Systems & Control Letters*, vol. 22, no. 2, pp. 123–129, 1994.

[12] Z. Wang, D. W. C. Ho, and X. Liu, "Variance-constrained filtering for uncertain stochastic systems with missing measurements," *IEEE Transactions on Automatic Control*, vol. 48, no. 7, pp. 1254–1258, 2003.

[13] C. K. Chu and G. Chen, *Kalman Filtering with Real-Time Applications*, 4th ed. Springer, 2009.

[14] S. J. Julier and J. K. Uhlmann, "A new extension of the Kalman filter to nonlinear systems," in *Int. Symp. Aerospace/Defense Sensing, Simul. and Controls*, vol. 3, no. 26, 1997, pp. 182–193.

[15] M. I. Ribeiro, *Kalman and Extended Kalman Filters: Concept, Derivation and Properties*. Institute for Systems and Robotics, Instituto Superior Tecnico, 2004.

[16] S. J. Julier and J. K. Uhlmann, "Unscented filtering and nonlinear estimation," *Proceedings of the IEEE*, vol. 92, no. 3, pp. 401–422, 2004.

[17] J. H. Wilkinson, *The Algebraic Eigenvalue Problem (Vol. 87)*. Clarendon Press Oxford, 1965.